

Platform-Motion Compensation for Velocity Measured by Doppler Lidar

Reginald J. Hill, Wm. Alan Brewer, Sara C. Tucker
 Cooperative Institute for Research in the Environmental Sciences / University of Colorado
 and
 Earth Systems Research Laboratory / NOAA
 325 Broadway
 Boulder, CO, USA 80303-3328
 Sara.Tucker@noaa.gov

INTRODUCTION

The NOAA Earth System Research Laboratory (ESRL) has developed two coherent Doppler lidar systems that have been deployed onboard research vessels to perform wind measurements during 8 field studies since 1998. Twenty-foot seagoing cargo containers (seatainers) house the systems and serve as mobile laboratories. Because the instruments measure the wind velocity relative to the motion of the lidar, correction for the motion of the platform is required. This is a synopsis of our journal paper.¹ That paper gives a thorough analysis of the correction for lidar velocity measurements. That analysis is general enough to be applied to Doppler velocity measurements from all monostatic ship- and aircraft-borne lidars and radars, and generalization to bistatic systems is doable. The correction is demonstrated here using mini-MOPA Doppler velocity data obtained during the Rain In Cumulus over the Ocean (RICO) experiment.

Typically, ESRL Doppler lidars perform low-elevation-angle scans to determine wind speed and direction and to quantify turbulence with high temporal and vertical resolution. This is accomplished by operating with a high pulse repetition frequency and controlling the direction of the lidar beam with a hemispheric scanner. The ESRL Doppler lidars use coherent detection to measure the radial velocity component of atmospheric scatterers (e.g., aerosol) relative to the velocity of the lidar.

THE MINI-MOPA DOPPLER LIDAR

To illustrate the effect of ship motion on the Doppler measurement, we focus on the ESRL mini-MOPA (master-oscillator power-amplifier) Doppler lidar for this paper. A simplified block

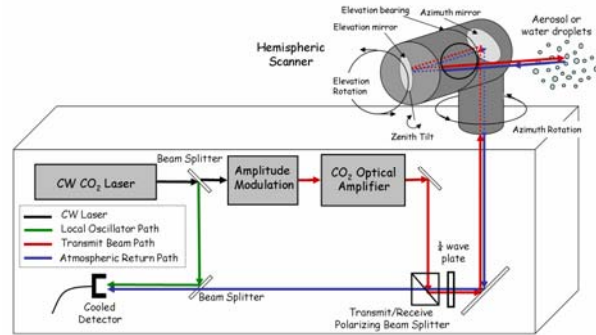


Figure 1. A simplified schematic of the lidar. Only a few optical elements, essential to the explanation, are shown.

diagram of the mini-MOPA Doppler lidar is shown in Fig. 1.

The lidar consists of a continuous wave (CW) carbon dioxide laser that provides both the local oscillator (LO) reference beam for heterodyne detection as well as the transmitted beam. The laser operates at a wavelength of 9.4 μm . Using the MOPA configuration, amplitude modulation is applied to the CW beam to chop out pulses. The pulse width produced by the modulation is adjustable. We typically operate with a pulse width of 400 ns (60m) when staring at zenith and 1 μs (150 m) when scanning. Each pulsed beam passes through a CO₂ optical amplifier to increase the pulse energy to 1 millijoule. In Fig. 1, the black and green beam paths are CW; green is the LO path, and the red and blue beam paths are pulsed beams. A polarizing beam splitter and quarter-wave plate are used as a transmit-receive (TR) switch. This allows common beam-steering optics to be used for both the transmitted and received beams. The transmitted beam is circularly polarized; its diameter is 20 cm, and it has a diffraction limited divergence of approximately 50 μrad . The lidar operates with a pulse repetition frequency of 200

to 300 Hz. The received beam passes through the hemispheric scanner and TR switch and is combined with the LO reference beam and is focused on a photo detector cooled by liquid nitrogen. Using heterodyne detection, the photo detector responds to the frequency difference between the reference beam (LO) and the atmospheric return. That frequency difference is the measured Doppler shift caused by the relative motion of atmospheric scatterers and the lidar system.

The transmitted beam is directed into the atmosphere using the hemispheric scanner that contains two mirrors; see Fig. 1. The scanner allows the lidar beam to probe the hemisphere above the seatainer by means of the "azimuth rotation" and "elevation rotation & tilt" shown in Fig.1. The elevation mirror is the final mirror before output of the beam to the atmosphere. The lidar has many more optical components than are shown in the block diagram in Fig. 1.

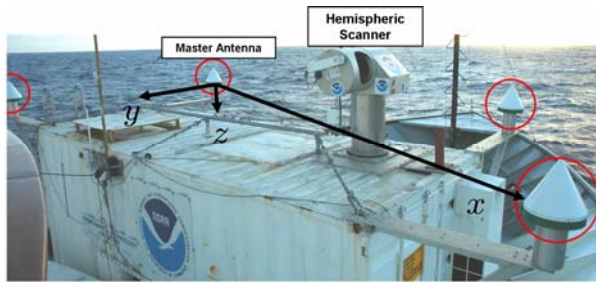


Figure 2. The lidar seatainer is shown deployed near the bow of the R/V Seward Johnson. The 4 GPS antennas of the MCS are encircled in red. The axis directions and origin of the lidar's coordinate system are indicated in black; x and y directions are in the plane of the antennas, and the z direction is perpendicular to that plane. Positions of the hemispheric scanner and the GPS master antenna are indicated.

To compensate for ship motion, a motion compensation system (MCS) performs two functions. The MCS actively stabilizes the pointing of the lidar beam, and computation using its data removes the effect of the ship motion from the Doppler wind measurement. To study boundary layer dynamics, the atmospheric velocity relative to an Earth-fixed coordinate system is desired. The MCS uses the Global Positioning

System (GPS) to define the Earth-fixed coordinate system and to determine the velocity, position, and rotation rate of the lidar relative to the GPS Earth-fixed coordinate system. See the caption of Fig. 2.

We show data from another motion detection system that was aboard the R/V Seward Johnson, namely the Position and Orientation System for Marine Vessels (POS MV). Cartesian axes of the POS MV's coordinate system are fixed relative to the ship and are oriented forward, starboard, and keelward, in that order.

MATHEMATICS OF THE MOTION CORRECTION

As viewed from an inertial reference frame as well as from the Earth's non-inertial GPS coordinate system, the many optical elements in the lidar and its scanner are in accelerated motion. We give a general derivation of the correction of Doppler measurements of velocity. Unfortunately that derivation is too lengthy to include in these 4 pages. The derivation is available.¹² Here we describe the mathematics.

The derivation relies on 3 facts: 1) the speed of light greatly exceeds all other relevant velocities; 2) the instrument's translation motion, and rotation rate are negligible during the time required for light to travel from the source to the scatterers and back to the detector; 3) the many optical elements comprising the lidar are constrained to two rigid bodies, namely the seatainer and the hemispherical scanner; 4) frequencies and wave vectors of light observed in one inertial reference frame are not the same as those observed in another inertial reference frame, but they are related by the non-relativistic Doppler shift formula.

Our derivation demonstrates that: i) for reflections from an arbitrary number of mirrors (or beam splitters, etc.) constrained to a rigid body, only the velocity of the last mirror relative to the source determines the frequency difference between the source and output beams; ii) applying that, the frequency shift from source to output to the atmosphere depends on the velocity, relative to the source, of the elevation mirror in Fig. 1; iii) similarly for the return path of scattered light, the frequency shift from input from the atmosphere to the detector depends on the velocity, relative to the

detector, of the elevation mirror in Fig. 1; iv), for a light path entirely within a rigid body, specifically the LO path in Fig. 1, the frequency of the source as observed in the source's inertial reference frame (i.e., moving with the same instantaneous velocity as the source) equals the frequency of the LO beam at the detector as observed in the detector's inertial reference frame; v) combining the aforementioned results with the non-relativistic Doppler shift formula relates the measured Doppler frequency shift to the Doppler shift caused by atmospheric scattering; that correction depends on the inner product of a wave-vector difference with the velocity relative to the detector of the elevation mirror; the wave-vector difference is approximated; vi) all of the foregoing is used to express the radial component of the velocity of atmospheric scatterers in the Earth's GPS coordinate system in terms of the measured Doppler shift and the corresponding radial component of the velocity of the elevation mirror; vii) the final desired motion-correction formula includes the fact that the MCS reports the velocity of the GPS 'master antenna' shown in Fig. 2 (and the POS MV reports at a point 22 m aft of the scanner). To calculate the velocity of the elevation mirror we use the MCS velocity (or POS MV-point velocity), the instantaneous position vector between the elevation mirror and master antenna (or POS MV point), and the rotation-rate vector of the seatainer (and ship).

MOTION CORRECTED RICO DATA

The motion correction is illustrated using zenith stare data from RICO. The hemispherical scanner maintains the pointing of the lidar beam to within 0.5 degrees despite the motion of the ship; thus the vertical component of velocity is measured in zenith stare mode.

Figure 3 (upper panel) shows the signal to noise ratio (SNR) for a 15-minute time segment during RICO. A cloud base is evident from the patch of enhanced SNR at 2 km altitude. Also in Fig. 3 are 3 vertical-velocity components in GPS coordinates as calculated from the lidars' MCS data during two minutes within the 15-minute segment. Figure 4 shows uncorrected and corrected vertical-velocity components obtained by application of the lidar's MCS data. The ship's

motion produces vertical stripes in the uncorrected data that are effectively removed by the correction.

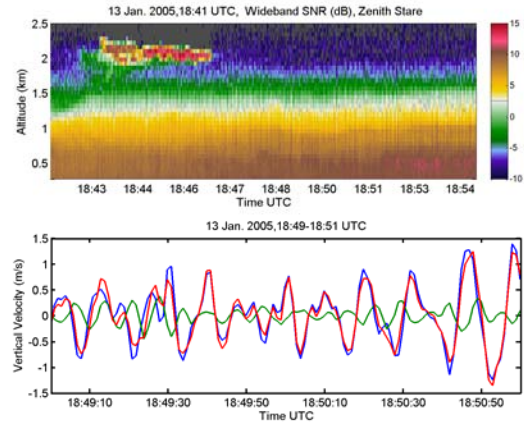


Figure 3. The upper panel shows signal-to-noise ratio for a zenith stare segment of data from RICO. A cloud base is evident on the left-hand side. The lower panel shows the GPS master-antenna's vertical-velocity component in blue, the vertical-velocity correction for the spatial separation between the master antenna and elevation mirror in green, and the elevation mirror's vertical-velocity component in red; all are obtained from the lidar's MSC data.

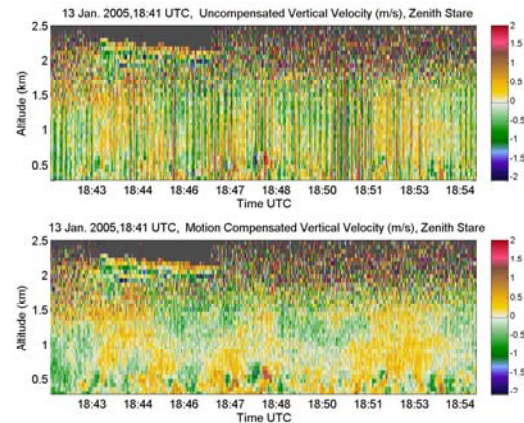


Figure 4. The uncorrected vertical-velocity component corresponding to the zenith stare of Fig. 3 is shown in the upper panel, and the corrected vertical-velocity component is in the lower panel.

Figure 5 (upper panel) shows SNR for 18 minutes during RICO when more clouds and rain were present relative to Fig. 3. Figure 5 (lower

panel) shows vertical-velocity components during the first two minutes of data in the upper panel as obtained from both the lidar's MCS and the ship's POS MV. Because the MCS's master antenna and the scanner are on opposite sides of the ship's roll axis, the vertical-velocity correction from the lidar's MCS is caused more by variation of the ship's roll than by variation of pitch or heading. In contrast, the scanner is nearly straight forward (in the ship's coordinate system) from the point where the POS MV gives its data; hence, variation of the ship's pitch mostly determines the vertical-velocity correction from the POS MV data. Despite those differences, Fig. 5 shows that the calculated vertical-velocity component of the elevation mirror is nearly the same for both the MCS and POS MV systems. Figure 6 shows the uncorrected and corrected vertical-velocity components obtained by use of the lidar's MCS data. Data in Fig. 6 correspond to the same 18 minutes as is shown in Fig. 5. Note the strong downward velocity caused by rain. The ship's motion is effectively removed by the motion correction.

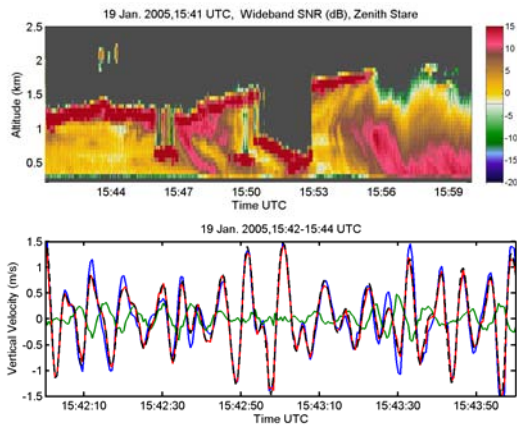


Figure 5. The upper panel shows signal-to-noise ratio for a zenith stare segment of data from RICO. Cloud bases and rain events are evident. The lower panel shows the GPS master-antenna's vertical-velocity component in blue, the vertical-velocity correction for the spatial separation between the master antenna and elevation mirror in green, and the elevation mirror's vertical-velocity component in red; all are obtained from the lidar's MCS data. The elevation mirror's vertical-velocity component, as determined from the ship's POS

MV data, is shown as black dashes (which obscure the red).

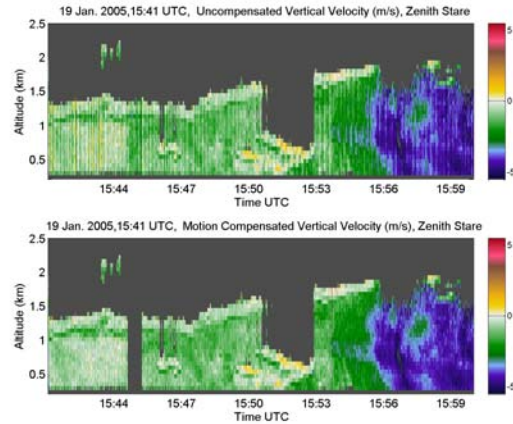


Figure 6. The uncorrected vertical-velocity component corresponding to the zenith stare of Fig. 5 is shown in the upper panel, and the corrected vertical-velocity component is in the lower panel. The large downward velocity at the right-hand side is caused by a rain event.

SUMMARY

We performed a detailed analysis of the correction of the Doppler shift for the shipboard motion of the lidar as well as rotation of its hemispheric scanner. We illustrate the efficacy of the correction in our figures. That efficacy shows that it is possible to use a ship's navigation system for the purpose of motion correction.

ACKNOWLEDGEMENTS

This work was supported in part by NSF grants ATM-0342647 and ATM-0342623.

REFERENCES

- ¹ Hill, R. J., W. A. Brewer, and S. C. Tucker, "Platform-Motion Correction of Velocity Measured by Doppler Lidar," (submitted to *J. Atmos. Ocean. Tech.*) (2007)
- ² Hill, R. J., "Correction of the Doppler Velocity of the NOAA Mini-MOPA Lidar for Ship Motion," NOAA Technical Memorandum OAR PSD-308. (Available from the National Technical Information Service, 5298 Port Royal Road, Springfield, VA 22161). (2005)